

**Title:** Graphene Oxide-based Biosensing Platform for Rapid and Sensitive Detection of HIV-1 Protease

**Author:** Youwen Zhang, Xiaohan Chen, Golbarg M Roozbahani, and Xiyun Guan\*

**Author affiliation:**

Department of Chemistry, Illinois Institute of Technology, 3101 S Dearborn St, Chicago, IL 60616, USA

**\*Corresponding author:**

Xiyun Guan  
Department of Chemistry  
Illinois Institute of Technology  
3101 S Dearborn St, Chicago, IL 60616, USA  
Tel: 312-567-8922; Fax: 312-567-3494  
E-mail: xguan5@iit.edu

## ABSTRACT

HIV-1 protease is essential for the life-cycle of the human immunodeficiency virus (HIV), and is one of the most important clinical targets for antiretroviral therapies. In this work, we developed a graphene oxide (GO)-based fluorescence biosensing platform for the rapid, sensitive and accurate detection of HIV-1 protease, in which fluorescent labeled HIV-1 protease substrate peptide molecules were covalently linked to GO. In the absence of HIV-1 protease, fluorescein was effectively quenched by GO. In contrast, in the presence of HIV-1 protease, it would cleave the substrate peptide into short fragments, thus producing fluorescence. Based on this sensing strategy, HIV-1 protease could be detected at as low as 1.18 nanogram per milliliter. More importantly, the sensor could successfully detect HIV-1 protease in human serum. Such GO-based fluorescent sensors may find useful applications in many fields, including diagnosis of protease-related diseases, as well as sensitive and high-throughput screening of drug candidates.

**Keywords:** HIV-1 Protease, Graphene Oxide, Biosensing, Human serum

## INTRODUCTION

Since the first cases of Acquired Immunodeficiency Syndrome (AIDS) were reported on June 5, 1981, human immunodeficiency virus (HIV) has caused nearly 30 million deaths [1]. At present, approximately 1.1 million people are infected with HIV in the United States. Among them, ~ 166,000 people are unaware of their status; and 30% of new HIV infections are transmitted by people who are living with undiagnosed HIV. Although effective HIV prevention strategies are useful to reduce the spread of HIV, early and accurate detection of HIV infection is critical to public health. Such an analytical capability can not only protect the healthy population, but also help ensure that HIV-infected people receive prompt treatment to control the virus and to slow the progression, thus reducing mortality. The conventional methods for HIV detection are based on either the detection of the presence of antibodies that the patient's body makes against HIV [2,3] or direct molecular recognition of HIV and its components such as specific nucleic acid sequences or antigens [4-6]. Although these diagnostic techniques are highly sensitive, they are not user-friendly (e.g., require the use of sophisticated instruments, and need for highly-trained personnel). Furthermore, conventional HIV tests do not detect acute HIV infection because of the existence of a relatively long window period. For example, the antibody-based HIV testing has a window period of approximately 3-6 weeks after infection, antigen testing reduces the window period to about 16 days, while nucleic acid testing cuts the detection window to ~ 12 days. To further reduce the window period and to detect HIV at the earliest stage of viral infection, development of rapid and highly sensitive HIV-1 protease activity assay is currently under intensive investigation [7-9]. HIV-1 protease (HIV-1 PR), which is a 99-amino acid 10~12 kD retroviral aspartyl protease and only functions as a homodimer, is essential for the life-cycle of the human immunodeficiency virus as it cleaves newly synthesized polyproteins (e.g., Prgag and Prgag-pol) to create the mature protein components of

infectious HIV virions. Without effective HIV-1 protease, HIV virions remain non-infectious, and hence, HIV-1 protease is one of the most important clinical targets for antiretroviral therapies. Thus far, many methods have been developed for HIV-1 PR detection, including mass spectrometry [7], surface plasmon resonance (SPR) [8], impedance spectroscopy [10], electrochemical assay [11], and nanopore stochastic sensing [12]. However, although most of these methods report detection limits in the low picomolar range, they are not suitable for point-of-care applications due to the time-consuming procedures and/or use of expensive and complicated instruments (note that portable point-of-care diagnostics is desired in resource-limited settings or home-based self-testing). Therefore, it is still of prime importance to develop a simple, rapid and sensitive method for HIV-1 PR detection.

Fluorescence resonance energy transfer (FRET), which relies on the distance-dependent transfer of energy from a donor molecule to an acceptor molecule (usually both fluorescent dyes), is a widely used technique to study biomolecule conformational change and molecular interaction [13]. Meanwhile, due to the sensitivity, simplicity and reproducibility, various FRET-based chemical sensors and biosensors have been developed to detect a wide variety of analytes, including metal ions, nucleic acids, peptides, proteins, and proteases [14-17]. Unlike semiconductor quantum dots (QDs), which are excellent donor fluorophores, graphene oxide (GO), a novel two-dimensional one-atom-thick carbon material, has been demonstrated to be an efficient quencher for various fluorophores [18,19]. In one approach to constructing protease GO-based FRET sensor, a dye labeled peptide, which contains the core substrate of a protease, is employed as a linker by non-specific adsorption to connect the fluorescence donor and GO. For example, Zhang's group developed a FRET sensor for thrombin detection by attaching a fluorescein isothiocyanate (FITC)-labeled peptide to GO via  $\pi-\pi$  interactions [20], while

Ma and co-workers fabricated a similar GO-based FRET sensor to detect MMP-2 based on electrostatic interactions [21]. Although these sensors are easy to prepare, they suffer from limited applications due to the severe matrix effect [18].

In this work, by covalently conjugating 5-carboxyfluorescein labeled peptide (Pep-FAM) to the GO surface, we designed a GO-Pep-FAM biosensing platform to rapidly, sensitively, and accurately detect HIV-1 PR even in complex human serum matrices. The Pep-FAM peptide contained the core substrate sequence (SQNYPIVQ) for specific identification of HIV-1 PR [22]. Introducing a mini-polyethylene glycol (mini-PEG) linker not only provided HIV-1 PR more space to interact with the peptide substrate but also improved the resolution of this sensor: compared with the Pep-FAM peptide without containing mini-PEG, a four-fold increase in the signal-to-noise ratio was observed under acidic condition. Without HIV-1 protease, FAM is effectively quenched by GO. However, with the presence of HIV-1 protease in the solution, it will cleave the peptide substrate and release a short peptide fragment with FAM dye into the solution, thus producing fluorescence (Scheme 1). Based on this strategy, HIV-1 protease can be detected at as low as 1.18 ng/mL. More importantly, the sensor could accurately detect HIV-1 protease in human serum samples within 30 min. Such GO-based sensors should have broad practical applications in many important fields, such as diagnosis of protease-related diseases and high-throughput screening of drug candidates.

## MATERIAL AND METHODS

**Chemicals.** HIV-1 protease was ordered from BioVendor Lab (Brno, Czech Republic), while the FAM labeled HIV-1 protease substrate peptide with a sequence of NH<sub>2</sub>-Mini-PEG-CALNNSQNYPIVQK(FAM) (95.49% pure) was purchased from

Biomatik corporation (Wilmington, DE). All the other chemicals were obtained from Sigma-Aldrich (St. Louis, MO). All the chemicals including HIV-1 protease and the substrate peptide were dissolved in HPLC-grade water (ChromAR, Mallinckrodt Baker). The stock solutions of the peptide and the protease were prepared at 1 mM and 200  $\mu$ g/mL, respectively, which were kept at -80 °C before and after immediate use. Two phosphate buffer saline (PBS) solutions were used in this study. One consisted of 1.0 M NaCl, 1 mM EDTA and 1 mM NaH<sub>2</sub>PO<sub>4</sub>, with the pH adjusted to 4.7 using H<sub>3</sub>PO<sub>4</sub>, while the other had a pH of 7.4, which contained of 10 mM phosphate, 138 mM NaCl and 2.7 mM KCl. The MES buffer comprised of 100 mM MES hydrate (pH 5.2).

**Instruments.** Fluorescence spectra were obtained by using a luminescence spectrophotometer (LS50B, PerkinElmer, Waltham, MA, USA). Infrared (IR) spectra were recorded with an infrared spectrophotometer (NEXUS 470 FT-IR, Thermo Nicolet, Waltham, MA, USA). The UV–Vis absorption spectra were obtained using a UV–Vis-NIR spectrophotometer (Varian Cary 500 Scan, Agilent, Santa Clara, CA, USA).

### **Preparation of graphene oxide (GO) conjugated biosensing platform**

The overall procedure of fabricating the HIV-1 protease sensor from graphene powder was summarized in Fig. 1, which consisted of three major steps.

**Preparation of GO.** GO was prepared using a modified Hummers method [23] with graphite powder as starting material. Briefly, five grams of graphite and 3.75g NaNO<sub>3</sub> were added into 375 mL of concentrated H<sub>2</sub>SO<sub>4</sub> (98%), and stirred for 1 hour. Then, KMnO<sub>4</sub> (22.5 g) was slowly added into the solution under an ice-water bath. The mixture was stirred for 3 days at 35 °C, followed by being heated to 90 °C and allowing the reaction to continue for another 2 hours. Next, 375 mL of water was added to the solution under

vigorous stirring, and cooled to 50 °C followed by stirring for another 30 min. The reaction was terminated by sequential addition of 15 mL H<sub>2</sub>O<sub>2</sub> solution and stirred for 10 min. Then, the mixture was washed with water under sonication. After centrifugation, the supernatant was removed and the precipitate was treated with 1 M HCl aqueous solution, and washed with water repeatedly until the pH of the solution reached 7.0. Finally, the product was freeze-dried after sonication for 150 min.

**Carboxylation of GO.** To increase the percentage of the carboxylic acid groups on the GO surface for better coupling of the peptide substrate, we treated GO with chloroacetic acid under strongly basic conditions to activate epoxide and ester groups, and to convert hydroxyl groups to carboxylic acid moieties [24]. Briefly, 40 mg GO was dissolved into 10 mL HPLC water, and then sonicated for 1 hour. Then, the GO suspension was mixed with 4.8 g NaOH and 4 g ClCH<sub>2</sub>COOH, and sonicated until the hydroxyl groups of GO were converted to carboxyl groups. The resultant solution was neutralized by HCl (1 M), and purified by repeated rinsing with water until carboxylated GO (GO-COOH) could be well dispersed in water [25].

**Preparation of the GO-Pep-FAM sensor.** The GO-Pep-FAM sensor for HIV-1 protease was prepared by covalently attaching the substrate peptide (Pep-FAM) of HIV-1 protease to GO-COOH. Briefly, GO-COOH (4 mg/mL, 37.5 μL) was dispersed in 10.0 mL of 2-(N-morpholino)-ethanesulfonic acid (MES) buffer (100 mM, pH 5.2). 76.680 mg of EDC (40 mM) and 21.713 mg of NHS (10 mM) were added to the GO-COOH suspension and sonicated for 30 min under an ice-water bath. The resulting mixture was centrifuged at 12,000 rpm for 10 min, and the supernatant was discarded. After washing the precipitate for three more times to remove excess EDC and NHS, it was dispersed in 10 ml

of PBS buffer (10 mM, pH 7.4). Then, 50  $\mu$ L Pep-FAM (1 mM) was added, and the mixture was stirred at room temperature for 2 hours in darkness. The product was purified by repeated centrifugation and rinsing with distilled water. The final product (with 53% yield) was dispersed in 10 mL water and stored in a refrigerator at 4 °C. Note that the reaction ratio of GO-COOH to Pep-FAM as described above was determined by incubating 5  $\mu$ M Pep-FAM with a series of GO-COOH solutions at different concentrations for 15 min followed by fluorescence measurement of the mixtures. As shown in Fig. S1 (see Electronic Supplementary Material), with an increase in the concentration of added GO-COOH, the fluorescence intensity of the Pep-FAM solution decreased rapidly until the concentration of GO-COOH reached 15  $\mu$ g/mL, at which the fluorescence quenching efficiency of GO-COOH was 73%. After that, the fluorescence signal decreased very slowly. The ratio of 5  $\mu$ M Pep-FAM to 15  $\mu$ g/mL GO-COOH was used to prepare the GO-Pep-FAM HIV-1 protease sensor since under this experimental condition, the fluorescence quenching efficiency of GO-COOH was relatively high, while the amount of GO-COOH consumed was relatively small.

## RESULTS AND DISCUSSION

### Characterization and optimization of GO-Pep-FAM sensor

**Infrared and UV-vis spectroscopy.** The chemical structures of GO, GO-COOH and conjugated GO-peptide (GO-Pep-FAM) samples were confirmed by infrared spectroscopy (FT-IR). As shown in Fig. 2a, characteristic absorption peaks appeared at 3400  $\text{cm}^{-1}$  (stretching vibration of -OH), 1700  $\text{cm}^{-1}$  (stretching vibration of C=O), and 1580  $\text{cm}^{-1}$  (stretching vibration of C=C), revealing the presence of -OH, C=O and C=C functional groups on GO. After activation of GO with chloroacetic acid, GO-COOH showed a stronger absorption band at 1634  $\text{cm}^{-1}$ , which indicated the formation of

carboxylate moieties  $\text{COO}^-$  in comparison with GO. After conjugation of peptides with GO-COOH, a strong characteristic band appeared at  $1650 \text{ cm}^{-1}$  (stretching vibration of CO-NH) with an increased small peak near  $2900 \text{ cm}^{-1}$  (stretching vibration of  $\text{CH}_2$ ), which indicated the successful formation of covalently linked GO-peptide. The significant difference between the structures of GO and GO-Pep-FAM was also supported by our UV-vis experiments. For example, as shown in Fig. 2b, the GO-Pep-FAM sample (0.01 mg/mL) had much larger absorbances in the visible region than GO (0.01 mg/mL), and showed a small peak at 480 nm, which was not observed in the GO sample. Furthermore, the color of the GO-Pep-FAM solution (1 mg/mL) was much darker than the GO solution at the same concentration (Fig. 2b, inset). Such a darkening phenomenon might be attributed to the restoring of the electronic conjugation within the graphene sheets [26,27]. As an important aside, we noticed that GO-Pep-FAM could be better dispersed in water than GO did. It is worth mentioning that, the good dispersibility of the GO-Pep-FAM sensor lays a foundation for its sensitive detection of HIV-1 protease. Taken together, the combined results supported our successful production of GO-Pep-FAM conjugate.

**Fluorescence spectra.** The fluorescence intensities of three samples (i.e., free HIV-1 PR substrate peptide Pep-FAM, mixture of GO-COOH and peptide Pep-FAM, and covalently-conjugated GO-Pep-FAM) were recorded with  $\lambda_{\text{ex/em}} = 490/513 \text{ nm}$ . Among them, the fluorescence signal of GO-Pep-FAM was the smallest (Fig. 2c). Since the same amount of Pep-FAM components were used in preparation of these samples, our experimental results demonstrated that the covalently attached GO was a more efficient quencher for Pep-FAM than the non-specific adsorption based GO-COOH. Hence, the GO-Pep-FAM sensor could detect HIV-1 protease more sensitively than the GO-COOH /

Pep-FAM mixture based HIV-1 PR sensor due to its smaller background fluorescence signal.

**pH effect.** To find an appropriate solution pH for sensitive detection of HIV-1 protease, the fluorescence intensities of the covalently-conjugated GO-Pep-FAM sensor and the mixture of GO-COOH and peptide Pep-FAM were investigated at a series of pH values ranging from 1 to 13. The experimental results were summarized in Fig. S2 (see Electronic Supplementary Material). We could see that, with an increase in the solution pH, the background fluorescence intensity of GO-Pep-FAM gradually increased (but didn't change much), while that of the mixture of GO and Pep-FAM increased drastically. Hence, the effect of the solution pH on Go-Pep-FAM was much less significant than that on GO-COOH / Pep-FAM mixture. Furthermore, since the covalently conjugated GO-Pep-FAM sensor had a smaller background fluorescence intensity than the non-specific adsorption-based GO / Pep-FAM mixture sensor at all the pH values investigated, GO-Pep-FAM is more suitable as a highly sensitive sensing element for HIV-1 protease detection. It should be noted that, the reason why solution pH affected the fluorescence intensity of GO-Pep-FAM is because fluorescein has multiple pH dependent ionic equilibria. Specifically, fluorescein has four species: cation, neutral, monoanion, and dianion. Among them, only the monoanion (quantum yield: 0.37) and dianion (quantum yield: 0.93) are fluorescent [28]. As the solution pH increased from 1 to 13, the dominant species of fluorescein changed from cation to neutral, monoanion, and dianion, gradually, thus affecting the fluorescence intensity of the sensor.

**HSA effect.** As described in the introduction section, in addition to the covalent conjugation approach, fluorescence can also be quenched by the  $\pi-\pi$  stacking and/or

electrostatic interaction between GO and labeled peptides. However, these types of non-specific absorption-based FRET sensors are unstable and can be easily disturbed when other similar molecules, especially proteins, competitively bind to GO. Therefore, investigation of the stability of the sensor (i.e., resistance to the competitive binding by proteins) can serve as a convenient means to evaluate whether the sensor was constructed with covalent coupling or via strong non-specific absorption. This process is similar to what was reported by Ratajczak et al, where fluorescein isothiocyanate (FITC) interacted nonspecifically with GO, resulting in its fluorescence quenching. However, this quenching was reduced in the presence of ATP because it would bind to GO via  $\pi$ - $\pi$  interactions, which replaced FITC from the GO surface [29]. For this purpose, a series of human serum albumin (HSA, an abundant serum protein) solutions with different concentrations was incubated with the GO-Pep-FAM sensor and the GO / Pep-FAM mixture, respectively, for 40 min at room temperature. The change ( $\Delta F$ ) in the fluorescence intensity of GO-Pep-FAM and GO / Pep-FAM mixture before and after addition of HSA was plotted against the concentration of HSA. As shown in Fig. 3, with an increase in the concentration of added HSA, the fluorescence intensity increased drastically for the GO / Pep-FAM mixture, suggesting the displacement of peptide from GO surface by HSA. Consequently, the non-specific absorption-based GO sensor is not suitable for analysis of samples with complicated matrices. In contrast, the fluorescence intensity of the GO-Pep-FAM suspension showed only a slight increase even when the concentration of HSA was increased to as high as 1000  $\mu$ g/mL, indicating the stability of GO-Pep-FAM against the adsorption of HSA on GO. These comparison results gave further evidence that our developed GO-Pep-FAM sensor was constructed via covalent bonding rather than non-specific absorption.

## Sensitivity and selectivity of the HIV-1 protease GO-Pep-FAM sensor

According to the literature [8], the optimum solution pH for enzymatic cleavage of the peptide substrate by HIV-1 protease was pH 4.7. In order to achieve highly sensitive detection of HIV-1 PR, the effect of GO-Pep-FAM concentration on HIV-1 PR detection was investigated. Briefly, three different concentrations (2  $\mu$ g/mL, 4  $\mu$ g/mL, and 8  $\mu$ g/mL) of GO-Pep-FAM suspension solutions (in PBS buffer, pH 4.7) were incubated with HIV-1 PR (100 ng/mL) for 40 min at 37 °C, followed by measuring their fluorescence intensity with  $\lambda_{\text{ex/em}} = 490/513$  nm (note that previous studies has shown that linearity deviation began to occur when GO concentration reached 17  $\mu$ g/mL [30]). Although an increased fluorescence intensity was obtained with an increase in the GO-Pep-FAM concentration (data not shown), 2  $\mu$ g/mL GO-Pep-FAM suspension solution was chosen to construct the dose-response curve for HIV-1 PR since it produced enough fluorescence signal without consuming too much GO-Pep-FAM. As shown in Fig. 4, the fluorescence intensity of the HIV-1 PR sample increased with an increase in the concentration of added HIV-1 protease, indicating that the peptide substrate (NH<sub>2</sub>-Mini-PEG-CALNNNSQNYPIVQK(FAM)) linked to the GO surface was being cleaved by HIV-1 protease. It was worth mentioning that the GO-based HIV-1 protease sensor not only had a wide dynamic range (linear regression with the HIV-1 protease concentration ranging from 5 to 300 ng/mL,  $R^2 = 0.9999$ ), but also was highly sensitive. The detection limit (which is defined as the dimeric HIV-1 protease concentration corresponding to three times the standard deviation of blank signal) of the sensor was 1.18 ng/mL (equivalent to 109 pM). To our best knowledge, such a detection limit, although not as impressive as that (10 pg/mL) of SPR, was comparable with those of other various HIV-1 protease sensors previously reported [7,8,11,12]. This detection limit is more than good enough for carrying out HIV-1 protease activity assay and inhibition study, where nanomolar concentrations of HIV-1 PR are routinely used [25,31].

Three proteases found in human serum, including matrix metalloproteinases 9 (MMP-9), trypsin, and prostate protein antigen (PSA), were selected as potential interfering species to examine the cross-reactivity of the GO-Pep-FAM sensor. In addition, since the HIV-1 protease standard contained Tris (20 nM), 2-(N-morpholino)ethanesulfonic acid (MES, 20 nM), Glycerol (10% v/v), and 2-Mercaptoethanol ( $\beta$ ME, 0.05% v/v), their interactions with the GO-Pep-FAM sensor were also investigated. Our experimental results (Fig. 4b) showed that the three protease samples (100 ng/mL each) had similar fluorescence intensities to those of the control (i.e., PBS buffer of pH 4.7) and other species, and all of them produced significantly smaller fluorescence signals than HIV-1 protease, thus suggesting the high specificity of our sensor.

### Simulated clinical sample analysis

**Effect of serum on HIV-1 protease detection.** To investigate whether serum would interfere with GO-Pep-FAM detection of HIV-1 PR, different volumes of human serum were mixed with GO-Pep-FAM suspension solution (prepared in PBS buffer, pH 4.7), followed by addition of HIV-1 PR (final concentration: 100 ng/mL), and incubated for 40 min at 37 °C. The fluorescence intensities of the serum / GO-Pep-FAM mixtures before and after addition of HIV-1 PR were recorded and summarized in Fig. 5. Our experimental results showed that the peptide substrate attached to the GO surface could still be efficiently cleaved by HIV-1 protease in the presence of serum matrix. However, serum did affect sensor performance and sensitivity. Specifically, as the volume of added serum increased from 10  $\mu$ L to 100  $\mu$ L, the noise (i.e., the background fluorescence intensity before addition of HIV-1 PR) of the GO-Pep-FAM sensor increased from 21.4 to 78.1, while the sensor signal (i.e., the fluorescence intensity after addition of HIV-1 PR) increased from 139.4 to 415.2. Therefore, with an increase in the serum volume, the

sensor sensitivity increased, while the signal-to-noise ratio (i.e., a measure of detection limit) of the sensor decreased (from 6.5 to 5.3). One likely reason why the existence of serum in the sample matrix would result in a significant increase in the fluorescence intensity was the effect of serum proteins on the GO-Pep-FAM sensor. For example, in the absence of serum, the fluorescently labeled peptide fragment (i.e., PIVQK-FAM) produced by HIV-1 PR cleavage of the substrate might be absorbed on the GO surface, leading to a loss of fluorescence signal. In contrast, in the presence of serum, serum proteins could competitively bind to GO, preventing the released peptide fragment being absorbed on the GO surface and hence restoring fluorescence. To support this interpretation, 50 ng/mL HIV-1 PR was analyzed by the GO-Pep-FAM sensor in the presence of HSA with different concentrations. Our experimental results (see Electronic Supplementary Material Fig. S3) showed that the fluorescence intensity did increase as the concentration of HSA increased. 50  $\mu$ L human serum was used in the remaining simulated clinical sample investigations since the GO-Pep-FAM sensor had both high sensitivity and good signal-to-noise ratio for HIV-1 PR detection under this experimental condition.

**Effect of incubation time on HIV-1 PR detection.** To optimize the reaction time for HIV-1 PR digestion of the peptide substrate in the presence of serum matrix, a mixture sample was prepared, which contained 50  $\mu$ L human serum and 1.45 mL GO-Pep-FAM suspension (in PBS buffer, pH 4.7). The mixture sample was then incubated with (100 ng/mL) HIV-1 PR for a period of time ranging from 10 min to 50 min, and the fluorescence was recorded accordingly. As shown in Fig. S4 (see Electronic Supplementary Material), our experimental results showed that the fluorescence intensity of the system increased with an increase in the reaction time, until the signal began to saturate after 30 minutes,

indicating the completion of the enzymatic digestion. To achieve sensitive and rapid detection of HIV-1 PR, 30 min was chosen as the optimal reaction time for the followed simulated clinical sample analysis. As a comparison, the conventional ELISA protein assay requires overnight coating followed by time-consuming (several hours) incubation and wash procedures [32].

**Mock serum sample analysis.** As discussed in the previous section, the GO-Pep-FAM / HIV-1 PR sensor system showed significantly enhanced fluorescence intensity in the presence of human serum. One of the major reasons might be attributed to the competitive binding of serum proteins (such as HSA) to the GO surface. Therefore, in order to accurately detect HIV-1 PR in the serum sample, one strategy could be adopted, which involved addition of either a certain concentration of HSA or a certain volume of human serum to the HIV-1 PR standard solutions to construct a modified dose-response curve for HIV-1 PR. For the proof-of-concept demonstration, a series of serum-containing HIV-1 PR standard solutions was prepared, which was obtained by spiking HIV-1 PR with concentrations ranging from 5 to 100 ng/mL to 50  $\mu$ L human serum. These solutions were then mixed with GO-Pep-FAM (1.45 mL, in PBS buffer, pH 4.7) and incubated at 37 °C for 30 min. The fluorescence measurement results were summarized in Fig. 6. Our experiments showed that fluorescence intensities of these solutions were indeed linearly correlated with the concentrations of HIV-1 PR ( $R^2 = 0.9987$ ). Using this modified calibration curve, the concentrations of HIV-1 PR in various serum samples were successfully quantitated (Table 1).

**Advantages and disadvantages of the Go-Pep-FAM biosensing platform.** As discussed in the introduction section, at present, there are three major types of methods for HIV

detection, i.e., based on the detection of the presence of antibodies that the patient's body makes against HIV, direct molecular recognition of HIV and its components such as specific nucleic acid sequences or antigens, and measurement of the activity of HIV-1 protease. Compared with the conventional HIV diagnostic techniques (i.e., antibody, nucleic acid, or antigen- based detection), one of the major advantages of the protease-based HIV detection strategy is that it is possible to detect acute HIV infection so that not only effective HIV prevention interventions may be timely implemented, but also the HIV-infected people can receive prompt treatment to control the virus and slow the progression. Note that, thus far, two major approaches have been developed for protease detection: affinity-based methods and activity-based assay. The former usually employs an antibody to analyze protease abundance, while the latter typically use a synthetic substrate consisting of a short peptide of known sequence to identify a specific protease and detect its activity. Since the activities of protease are tightly regulated through post-translational modifications, these modifications typically occur in the absence of any detectable change in protease abundance and are thus invisible to the affinity-based protease assay, leading to significant difference between overall abundance levels and activity of proteases. In addition to the capability to detect acute disease infection, other advantages of measuring protease activities include inhibitor screening, and drug development. Among various HIV-1 PR detection methods reported thus far, although our developed GO-Pep-FAM sensor is not most sensitive, its detection limit is more than good enough for carrying out HIV-1 protease activity assay and inhibition study. Compared with most of the other HIV-1 PR detection methods using the expensive and sophisticated instrument, one significant advantage of our developed GO-based fluorescent sensor is its potential portable point-of-care HIV diagnostics in resource-limited settings or home-based self-testing.

## **CONCLUSION**

In conclusion, by covalently attaching fluorescently labeled HIV-1 protease substrate peptide molecules to the GO surface, a rapid and accurate FRET sensor for HIV-1 PR was successfully developed. In addition to its high sensitivity, small background noise level, and good detection limit (nanogram per milliliter), our developed GO-Pep-FAM sensor is robust (still functioned after 3 weeks, see Electronic Supplementary Material Fig. S5), and more resistant to the matrix disturbance than the non-specific adsorption-based FRET sensor. Furthermore, serum samples could be accurately analyzed. It can be visualized that the same GO-Pep-FAM sensing strategy can be utilized to develop highly sensitive and selective sensors for a variety of other proteases by changing the peptide substrates. These GO-based FRET sensors may find useful applications in many fields, including diagnosis of protease-related diseases, as well as sensitive and high-throughput screening of drug candidates.

## **Supplementary Material**

The supplementary material is available free of charge on the Publications website. Additional figures, including effect of GO-COOH concentration on fluorescence intensity and quenching efficiency, effect of solution pH on fluorescence intensities of GO-COOH / Pep-FAM mixture and GO-Pep-FAM, effect of HSA on GO-Pep-FAM detection of HIV-1PR, effect of reaction time on GO-Pep-FAM detection of HIV-1 PR, and effect of storage time of on GO-Pep-FAM detection of HIV-1 PR.

## **Acknowledgments**

This work was financially supported by the National Institutes of Health (2R15GM110632-02) and National Science Foundation (1708596).

## Compliance with ethical standards

**Conflict of interest** The authors declare that there is no conflict of interest.

## Figure Legends

**Scheme 1.** The principle of detecting HIV-1 Protease

**Fig. 1** Schematic representation of fabrication of HIV-1 protease sensor with graphene powder.

**Fig. 2** Characterization of GO-Pep-FAM sensor. (a) FT-IR spectra of GO, GO-COOH and GO-Pep-FAM; (b) UV-Vis spectra of GO and GO-Pep-FAM; and (c) fluorescence spectra of Pep-FAM, GO / Pep-FAM mixture, and covalently-conjugated GO-Pep-FAM. The concentrations of GO and GO-Pep-FAM used in Fig. 2b were 0.01 mg/mL each, while those of Pep-FAM, GO, and GO-Pep-FAM used in Fig. 2c were 5  $\mu$ M, 15  $\mu$ g/mL, 15  $\mu$ g/mL, respectively. All the solutions of Pep-FAM, GO, and GO-Pep-FAM were prepared in HPLC water.

**Fig. 3** Effect of HSA on (a) GO-Pep-FAM and (b) GO / Pep-FAM mixture. Experiments were performed by incubating GO-Pep-FAM suspension solutions (15  $\mu$ g/mL, in HPLC water) or mixtures of GO (15  $\mu$ g/mL, in HPLC water) and Pep-FAM (5  $\mu$ M, in HPLC water) with various concentrations of HSA for 40 min, followed by measuring their fluorescence intensity with  $\lambda_{\text{ex/em}} = 490/513$  nm at room temperature. Each data point represents the average from three replicate analyses  $\pm$  one standard deviation.

**Fig. 4** GO-Pep-FAM detection of HIV-1 protease. (a) Fluorescence spectra of GO-Pep-FAM in the presence of HIV-1 protease at various concentrations; and (b) plot of

fluorescence intensity versus analyte species, showing the selectivity of the GO-Pep-FAM sensor. The inset in Fig. 4a displays the dose-response curve for HIV-1 protease. Experiments were performed by incubating GO-Pep-FAM suspension solutions (2  $\mu$ g/mL, in PBS buffer, pH 4.7) with HIV-1 PR or other analyte species for 40 min at 37 °C, followed by measuring their fluorescence intensity with  $\lambda_{\text{ex/em}} = 490/513$  nm at room temperature. Each data point represents the average from three replicate analyses  $\pm$  one standard deviation.

**Fig. 5** Effect of human serum on GO-Pep-FAM detection of HIV-1 PR. Experiments were performed by mixing different volumes of human serum with GO-Pep-FAM suspension solution (2  $\mu$ g/mL, prepared in PBS buffer, pH 4.7), followed by addition of HIV-1 PR (100 ng/mL), and incubated for 40 min at 37 °C. Fluorescence intensities of these mixtures were recorded with  $\lambda_{\text{ex/em}} = 490/513$  nm at room temperature. Each data point represents the average from three replicate analyses  $\pm$  one standard deviation.

**Fig. 6** Simulated serum sample analysis. (a) Fluorescence spectra of GO-Pep-FAM in the presence of HIV-1 protease at various concentrations; and (b) plot of fluorescence intensity versus HIV-1 protease concentration. Experiments were performed by incubating GO-Pep-FAM suspension solutions (2  $\mu$ g/mL, in PBS buffer, pH 4.7) with various simulated human serum samples for 40 min at 37 °C, followed by measuring their fluorescence intensity with  $\lambda_{\text{ex/em}} = 490/513$  nm at room temperature. Each data point represents the average from three replicate analyses  $\pm$  one standard deviation.

## References

1. De Cock KM, Jaffe HW, Curran JW. Reflections on 30 years of AIDS. *Emerg Infect Dis.* 2011; 17:1044-8.
2. Laird GM, Eisele EE, Rabi SA, Lai J, Chioma S, Blankson JN, Siliciano JD, Siliciano RF. Rapid quantification of the latent reservoir for HIV-1 using a viral outgrowth assay. *PLOS Pathogens.* 2013; 9: e1003398.
3. Bhimji A, Zaragoza AA, Live LS, Kelley SO. Electrochemical enzyme-linked immunosorbent assay featuring proximal reagent generation: detection of human immunodeficiency virus antibodies in clinical samples. *Anal Chem.* 2013; 85: 6813-19.
4. Yan N, O'Day E, Wheeler LA, Engelman A, Lieberman J. HIV DNA is heavily uracilated, which protects it from autointegration. *Proc Natl Acad Sci USA.* 2011; 108: 9244-49.
5. Zhang DW, Zhao MM, He HQ, Guo SX. Real-time monitoring of disintegration activity of catalytic core domain of HIV-1 integrase using molecular beacon. *Anal Biochem.* 2013; 440: 120-2.
6. Palmer S, Wiegand AP, Maldarelli F, Bazmi H, Mican JM, Polis M, Dewar RL, Planta A, Liu S, Metcalf JA, Mellors JW, Coffin JM. New real-time reverse transcriptase-initiated pcr assay with single-copy sensitivity for human immunodeficiency virus type 1 RNA in plasma. *J Clin Microbiol.* 2003; 41: 4531-36.
7. Davis DA, Tebbs IR, Daniels SI, Stahl SJ, Kaufman JD, Wingfield P, Bowman MJ, Chmielewski J, Yarchoan R. Analysis and characterization of dimerization inhibition of a multi-drug-resistant human immunodeficiency virus type 1 protease using a novel size-exclusion chromatographic approach. *Biochem J.* 2009; 419: 497.
8. Esseghaier C, Ng A, Zourob M. A novel and rapid assay for HIV-1 protease detection using magnetic bead mediation. *Biosens Bioelectron.* 2013; 41 (Supplement C): 335-41.
9. Biswas P, Cella LN, Kang SH, Mulchandani A, Yates MV, Chen W. A quantum-dot based protein module for in vivo monitoring of protease activity through fluorescence resonance energy transfer. *Chem Commun.* 2011; 47: 5259-61.
10. Mahmoud KA, Hrapovic S, Luong JHT. Picomolar detection of protease using peptide/single walled carbon nanotube/gold nanoparticle-modified electrode. *ACS Nano* 2008; 2: 1051-57.
11. Mahmoud KA, Luong JHT. A sensitive electrochemical assay for early detection of

hiv-1 protease using ferrocene-peptide conjugate/Au nanoparticle/single walled carbon nanotube modified electrode. *Anal Lett.* 2010; 43: 1680-87.

12. Wang L, Han Y, Zhou S, Wang G, Guan X. Real-time label-free measurement of HIV-1 protease activity by nanopore analysis. *Biosens Bioelectron.* 2014; 62: 158-62.
13. Geim AK, Novoselov KS. The rise of graphene. *Nat Mater.* 2007; 6: 183.
14. Yang C, Yin X, Huan SY, Chen L, Hu XX, Xiong MY, Chen K, Zhang XB. Two-photon DNAzyme-gold nanoparticle probe for imaging intracellular metal ions. *Anal Chem.* 2018; 90: 3118-23.
15. Ma Q, Gao Z. A simple and ultrasensitive fluorescence assay for single-nucleotide polymorphism. *Anal Bioanal Chem.* 2018; 410: 3093-100.
16. Huang H, Li P, Zhang M, Yu Y, Huang Y, Gu H, Wang C, Yang Y. Graphene quantum dots for detecting monomeric amyloid peptides. *Nanoscale.* 2017; 9: 5044-48.
17. Liu Q, Li N, Wang M, Wang L, Su X. A label-free fluorescent biosensor for the detection of protein kinase activity based on gold nanoclusters/graphene oxide hybrid materials. *Anal Chim Acta.* 2018; 1013: 71-8.
18. Wang, H.; Zhang, Q.; Chu, X.; Chen, T.; Ge, J.; Yu, R. Graphene oxide-peptide conjugate as an intracellular protease sensor for caspase-3 activation imaging in live cells. *Angew Chem Int Ed.* 2011; 50: 7065-9.
19. Lu CH, Yang HH, Zhu CL, Chen X, Chen GN. A Graphene Platform for Sensing Biomolecules. *Angew Chem Int Ed.* 2009; 48: 4785-7.
20. Zhang M, Yin BC, Wang XF, Ye BC. Interaction of peptides with graphene oxide and its application for real-time monitoring of protease activity. *Chem Commun.* 2011; 47: 2399-401.
21. Feng D, Zhang Y, Feng T, Shi W, Li X, Ma H. A graphene oxide-peptide fluorescence sensor tailor-made for simple and sensitive detection of matrix metalloproteinase 2. *Chem Commun.* 2011; 47: 10680-82.
22. Perez MAS, Fernandes PA, Ramos MJ. Substrate Recognition in HIV-1 Protease: A Computational Study. *J Phy Chem B.* 2010; 114: 2525-32.
23. Stankovich S, Dikin DA, Dommett GHB, Kohlhaas KM, Zimney EJ, Stach EA, Piner RD, Nguyen ST, Ruoff RS. Graphene-based composite materials. *Nature* 2006; 442: 282.
24. Li D, Müller MB, Gilje S, Kaner RB, Wallace GG. Processable aqueous dispersions of graphene nanosheets. *Nature Nanotechnol.* 2008; 3: 101.
25. Ingr M, Uhlíková T, Strísovský K, Majerová E, Konvalinka J. Kinetics of the

dimerization of retroviral proteases: the "fireman's grip" and dimerization. *Protein Sci.* 2003; 12: 2173-82.

26. Hummers WS, Offeman RE. Preparation of graphitic oxide. *J Am Chem Soc.* 1958; 80: 1339-9.
27. Liu Z, Robinson JT, Sun X, Dai H. PEGylated nanographene oxide for delivery of water-insoluble cancer drugs. *J Am Chem Soc.* 2008; 130: 10876-10877.
28. Ferrari L, Rovati L, Fabbri P, Pilati F. Disposable fluorescence optical pH sensor for near neutral solutions. *Sensors.* 2012; 13:484-99.
29. Ratajczak K, Stobiecka M. Ternary interactions and energy transfer between fluorescein isothiocyanate, adenosine triphosphate, and graphene oxide nanocarriers. *J Phys Chem B.* 2017; 121:6822-30.
30. Stobiecka M, Dworakowska B, Jakiela S, Lukasiak A, Chalupa A, Zembrzycki K. Sensing of survivin mRNA in malignant astrocytes using graphene oxide nanocarrier-supported oligonucleotide molecular beacons. *Sens Actuators B Chem.* 2017; 235: 136-45.
31. Windsor IW, Raines RT. Fluorogenic assay for inhibitors of HIV-1 protease with sub-picomolar affinity. *Sci Rep.* 2015; 5: 11286.
32. Gutiérrez OA, Salas E, Hernández Y, Lissi EA, Castrillo G, Reyes O, Garay H, Aguilar A, García B, Otero A, Chavez MA, Duarte CA. An immunoenzymatic solid-phase assay for quantitative determination of HIV-1 protease activity. *Anal Biochem.* 2002; 307:18-24.

**Table 1.** Recovery of HIV-1 protease from serum by use of the Go-Pep-FAM sensor. Each value represents the mean of three replicate analyses  $\pm$  one standard deviation.

Sample number	Theoretical value (ng/mL)	Experimental value $\pm$ SD (ng/mL)
1	5	3.99 $\pm$ 0.93
2	10	12.0 $\pm$ 2.2
3	20	24.6 $\pm$ 1.3
4	40	37.7 $\pm$ 2.7
5	60	64.1 $\pm$ 1.9
6	80	80.0 $\pm$ 0.4
7	100	94.7 $\pm$ 3.0

Scheme 1

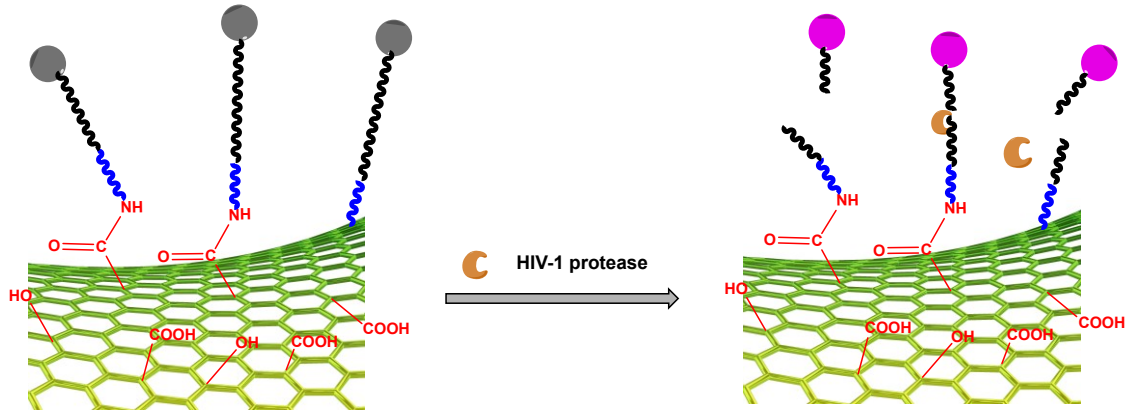


Figure 1

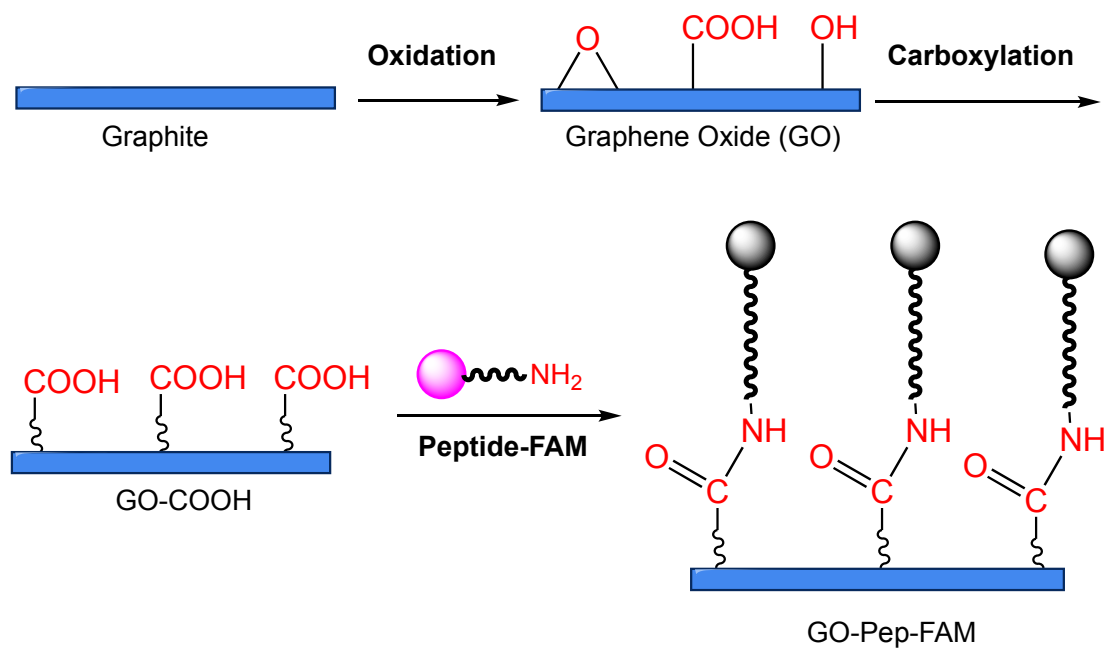


Figure 2

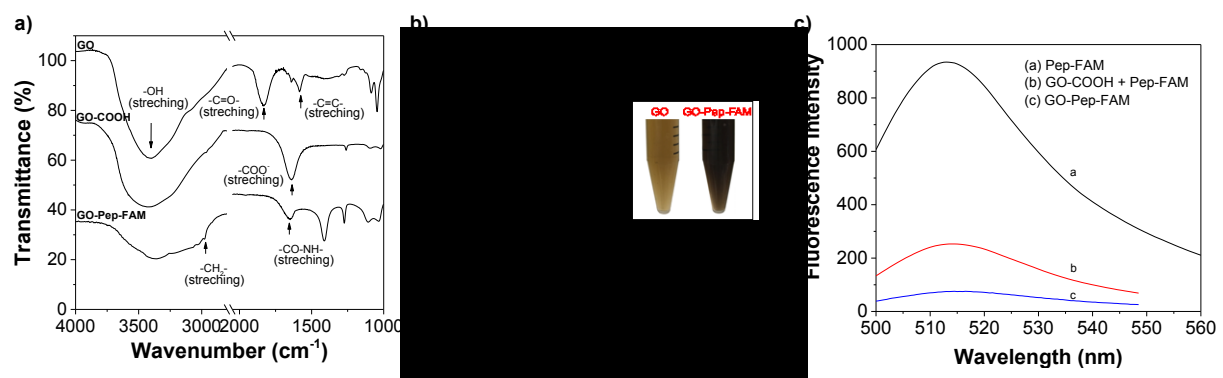


Figure 3

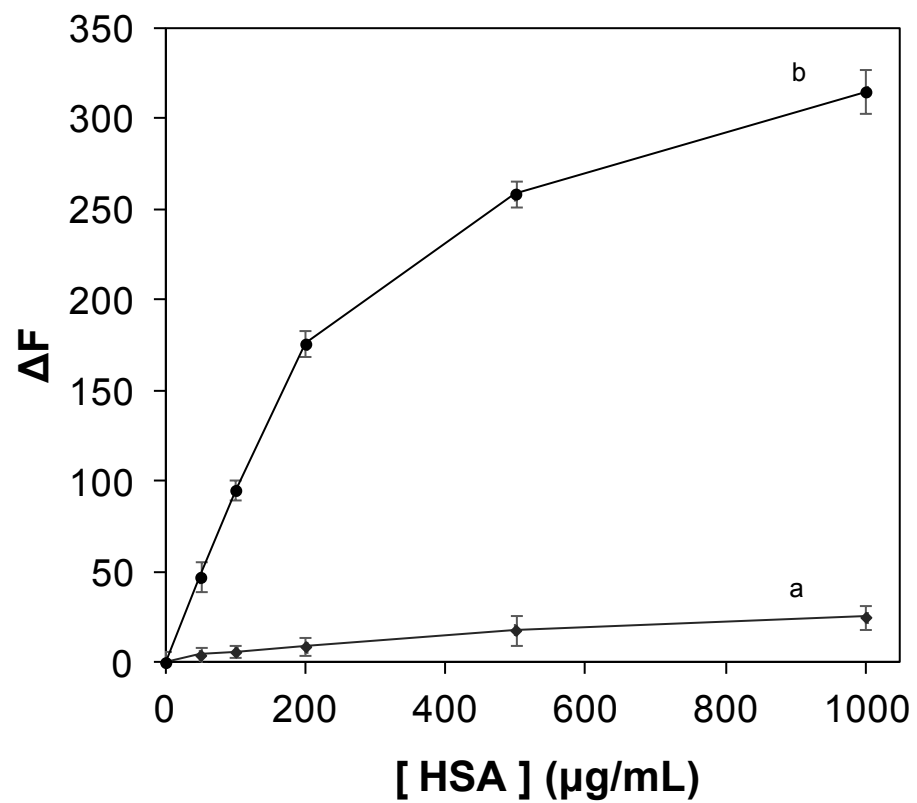


Figure 4

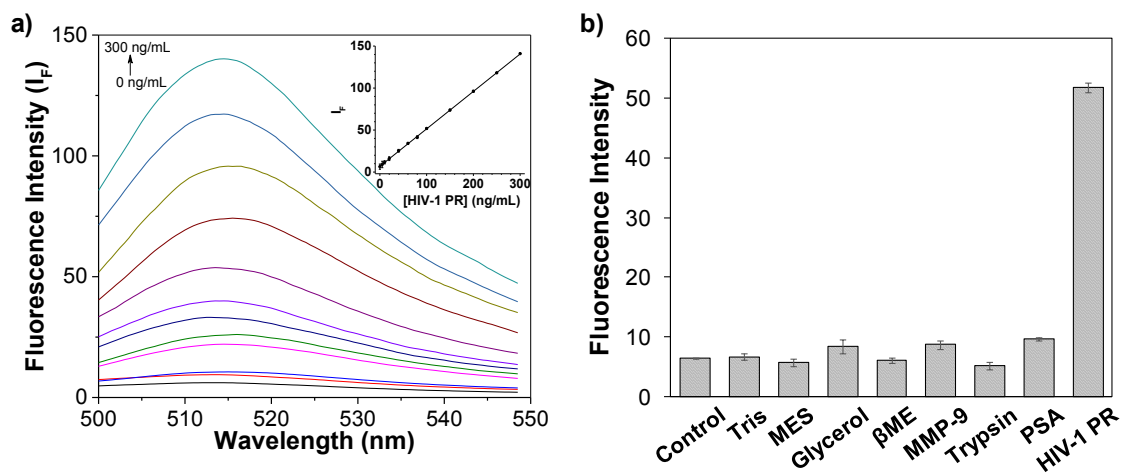


Figure 5

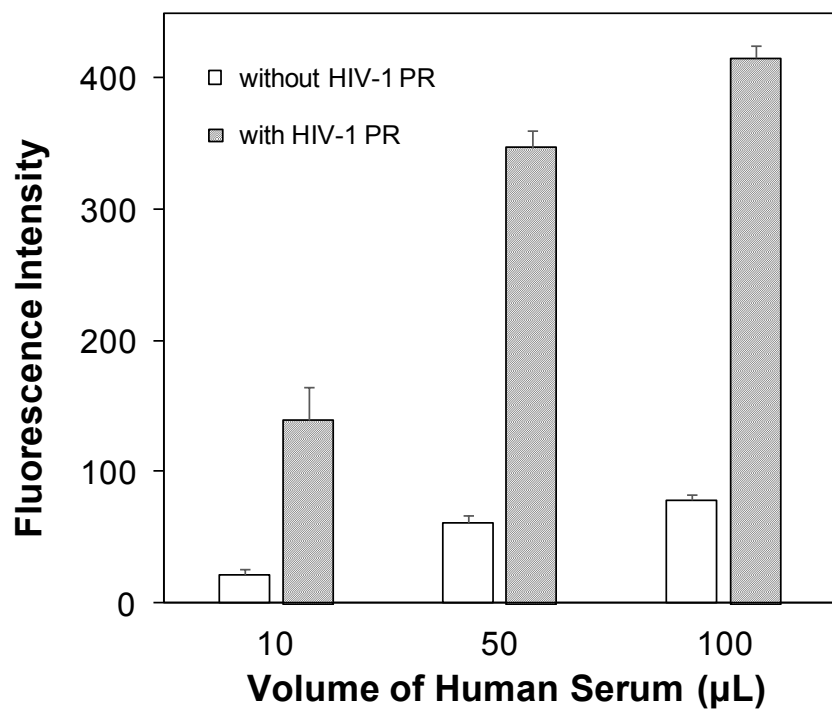
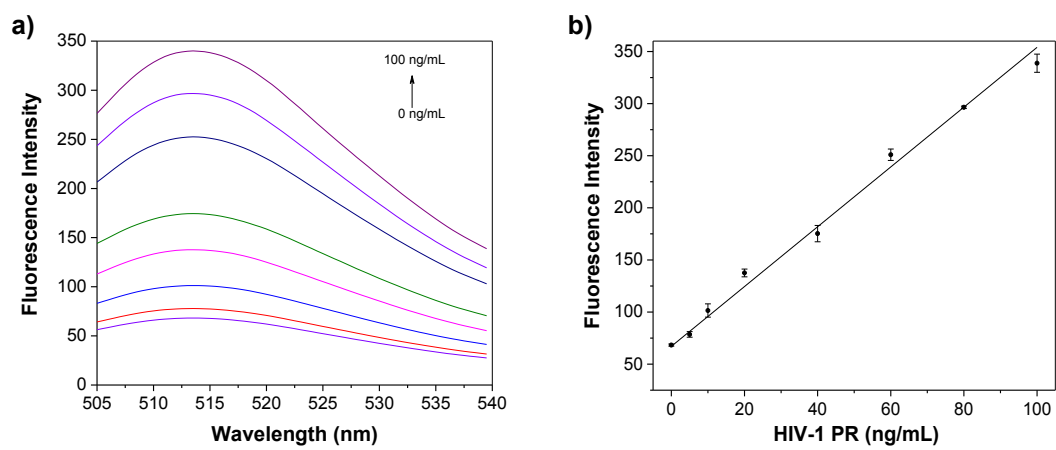


Figure 6



“For TOC Only” (Graphical Abstract)

